NONLINEAR CONTROL APPLIED TO AN AUTONOMOUS VEHICLE

CONTROL NO LINEAL APLICADO A UN VEHÍCULO AUTÓNOMO

Ariadna Berenice Flores Jiménez
Universidad de Guadalajara, Centro Universitario de la Ciénega, México
ariadna.flores9256@alumnos.udg.mx

Stefano Di Gennaro
University of L´Aquila, Italia
stefano.digennaro@univaq.it

Cuauhtémoc Acosta Lúa
Universidad de Guadalajara, Centro Universitario de la Ciénega, México
cuauhtemoc.acosta@academicos.udg.mx

Reception: 8/december/2024 **Acceptance**: 6/february/2025

Abstract

This paper addresses the problem of path tracking for a scaled vehicle AutoNOMO-mini. The formulation of this problem is analogous to the tracking control of a non-holonomic vehicle. Consequently, the kinematic model of the vehicle was considered. This study presents two control techniques applied to the scaled vehicle: the PID-like controller and the Sliding Mode Controller (SMC). Both controllers can regulate the direction of the vehicle to ensure it follows a specific trajectory. To evaluate their performance, the controllers were tested by measuring the steering angle of the front wheels of the scaled vehicle. The results demonstrated that the vehicle was capable of maintaining its intended trajectory. To demonstrate the feasibility of the approach, numerical simulations were performed in Matlab-Simulink and experimental tests were conducted on the AutoNOMO-mini vehicle.

Keywords: AutoNOMO-mini, Path Tracking, PID Control, Sliding Mode Control.

Resumen

Este artículo aborda el problema del seguimiento de trayectoria para un vehículo a escala AutoNOMO-mini. La formulación de este problema es análoga al control

de seguimiento de un vehículo no holonómico. Debido a esto, se considera el modelo cinemático del vehículo. Este estudio presenta dos técnicas de control aplicadas al vehículo a escala: el controlador tipo PID y el Controlador por Modos Deslizantes (SMC por sus siglas en inglés). Ambos controladores son capaces de regular la dirección del vehículo para asegurar que siga una trayectoria específica. Para evaluar su rendimiento, los controladores se probaron midiendo el ángulo de dirección de las ruedas delanteras del vehículo a escala. Los resultados demostraron que el vehículo fue capaz de mantener la trayectoria prevista. Para demostrar la viabilidad del enfoque, se realizaron simulaciones numéricas en Matlab-Simulink y se realizaron pruebas experimentales en el vehículo AutoNOMO-mini.

Palabras Clave: *AutoNOMO-mini, Control de Modos Deslizantes, Control PID, Seguimiento de trayectoria.*

1. Introduction

Autonomous ground vehicles are automobiles that operate without any human involvement. These vehicles utilize a combination of sensors, computer processors, and databases to effectively detect and identify their surrounding environments, plan their actions, navigate, and make informed decisions [Rajasekhar, 2015]. To ensure optimal performance, thorough study and testing are required. Miniature vehicles offer an economical and efficient method for conducting these experiments before launching full-sized vehicles. They closely resemble the motion and perception of their larger counterparts, providing a valuable means for evaluating the performance and functionality of autonomous vehicles in a controlled and cost-effective manner. The experiments presented in this article utilize the AutoNOMO-mini (see Figure 1). This vehicle is a 1:10 scale model designed for educational and research purposes. It is equipped with two cameras, including the Fish-Eye camera ELP 1080p and the Intel RealSense Depth Camera SR300, as well as various sensors, including a laser scanner (RPLIDAR), an Inertial Measurement Unit (MPU6050), and an encoder [Sanchez-Buelna, 2019].

Automobile-type robots, such as the AutoNOMO-mini, are underactuated nonlinear systems with nonholonomic constraints. Kinematic models often simplify the control design of these complex systems. This simplification is valid as long as the vehicle meets the assumption of rolling without slipping. Therefore, considering the two rear and front wheels to be situated at the center of their respective axles, the scaled vehicle can be modelled as a non-holonomic robot, Then, the transformation known as chained form can be applied in order to obtain its controllers in a simple way [De Luca, 1998]. On the other hand, a description and comparison of the kinematic and dynamic model of the bicycle for model-based control in autonomous driving can be found in [Kong, 2015]. For such vehicles, the primary control tasks are lateral and longitudinal control (steering and speed). The literature contains numerous references to different methods.

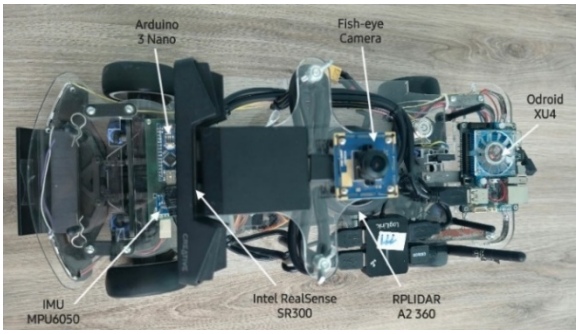

Source: authors

Figure 1 AutoNOMO–mini vehicle.

In [Kong, 2015] a comprehensive analysis is provided of the construction of a Model Predictive Control (MPC) system for autonomous vehicles, with a specific focus on the kinematic bicycle model. The paper [Zhejun, 2021] introduces a trajectory-tracking approach that utilizes Model Predictive Control. This approach uses backward Euler integration instead of the forward Euler integration method to create the prediction model. PID controllers, like the one developed in [Kebbati, 2021], are widely employed in various industries due to their excellent performance and straightforwardness. The essay talks about the longitudinal control task and suggests two ways to use adaptive PID control: GA-PID (genetic algorithms) and NN-PID (neural networks). The paper [Dong, 2021] suggests a data-driven control

algorithm for fractional-order PID (FOPID) control. The goal is to make it easier to follow the desired path while keeping the system stable. The paper [Tiwari, 2021] introduces an additional PID control system for maintaining a vehicle's cruising velocity (longitudinal control). It also presents a Stanley control system for accurately following a desired trajectory (lateral control). Furthermore, the paper referenced as [Farag, 2020] presents a proportional-integral-differential control method for autonomous cars to do track maneuvering.

The SMC is another technique for controlling autonomous vehicles. In [Sabiha, 2022], SMC is applied to vehicle dynamics to obtain the desired torques and drive the vehicle to the desired trajectory. In [Sekbah, 2023], three Adaptive Sliding Mode Controllers (A-SMC) based on dynamics for trajectory tracking are presented, aiming to outperform traditional SMC. In order to reduce transient errors between vehicle positions and the roadway, a sliding mode control based on a simplified bicycle model for lateral control is designed in [Milani, 2022]. Finally, in [Jiang, 2022], a backstepping sliding mode control based on kinematics and attitude deviations for AGVs (Automated Guided Vehicles) is proposed to address the trajectory following control problem.

2. Methods

Kinematic model

The AutoNOMO-mini is a robotic device that emulates the behavior of an automobile. Consequently, the kinematic model of the vehicle can be utilized. This model considers the car to be moving along an inertial frame with the steering of the vehicle being controlled by the front wheels, while the rear wheels maintain a fixed orientation. The representation of the vehicle in the inertial frame is illustrated in Figure 2.

Where $x \in R$ and $y \in R$ are the Cartesian coordinates, l is the distance between the front and rear wheels, θ and φ represent the orientation with respect to the x-axis and the steering angle, respectively. Considering the vehicle´s wheels restrictions and its lateral speed, Equations 1 and 2 are obtained. Where $\dot{x}$ and $\dot{y}$ represent the derivatives of the Cartesian coordinates (x, y).

$$\left(\dot{x} - l\,sin\,\theta\,\dot{\theta}\right) sin(\theta + \varphi) - (\dot{y} + l\,cos\,\theta\,\cos\,(\theta + \varphi)) = 0 \quad (1)$$

$$\dot{x}\,sin\,\theta - \dot{y}\,cos\,\theta = 0 \quad (2)$$

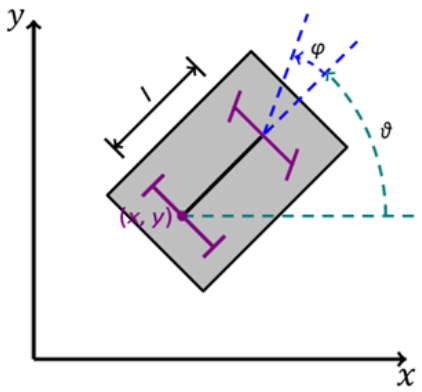

Source: authors

Figure 2 The kinematic model of the vehicle.

Equation 1 can be rewritten as Equation 3.

$$dx\,sin(\theta + \varphi) - dy\,cos(\theta + \varphi) - l(sin(\theta)\,sin(\theta + \varphi) + cos\,\theta\,cos(\theta + \varphi))\,d\theta = 0 \quad (3)$$

By applying trigonometric identities, Equation 3 can be reformulated as Equation 4.

$$sin(\theta + \varphi)\,dx - cos(\theta + \varphi)\,dy - l\,cos\,\varphi\,d\theta = 0 \quad (4)$$

Equations 2 and 4 can be rewritten as Equations 5 and 6.

$$w_1 = sin(\theta + \varphi)\,dx - cos(\theta + \varphi)\,dy - l\,cos\,\varphi\,d\theta \quad (5)$$

$$w_2 = sin\,\theta\,dx - cos\,\theta\,dy \quad (6)$$

Considering the linear velocity v_1 as $v_1 = \sqrt{\dot{x}^2 + \dot{y}^2}$, $\dot{x}$ and $\dot{y}$ can be expressed as shown in Equations 7 and 8.

$$\dot{x} = v_1\,cos\,\theta \quad (7)$$

$$\dot{y} = v_1\,sin\,\theta \quad (8)$$

Using trigonometric identities, Equation 5 can be rewritten as Equation 9.

$$(sin\,\theta\,cos\,\varphi + cos\,\theta\,sin\,\varphi)\,dx + (-cos\,\theta\,cos\,\varphi + sin\,\theta\,sin\,\varphi)dy = l\,cos\,\varphi\,d\theta \quad (9)$$

Multiplying Equation 9 by $1/cos\,\varphi$, one obtains Equation 10.

$$(sin(\theta) + cos(\theta)\,tan\,\varphi)\,dx + (-cos(\theta) + sin(\theta)\,tan\,\varphi)\,dy = l\,d\theta \quad (10)$$

Considering $w_2 = 0$ in Equation 6, Equation 10 can be rewritten as Equation 11.

$$tan\,\varphi\,(cos\,\theta\,\dot{x} + sin\,\theta\,\dot{y}) = l\dot{\theta} \tag{11}$$

Using the Equations 7 and 8 in Equation 11, one gets Equation 12.

$$tan\,\varphi\,(cos\,\theta\,v_1\,cos\,\theta + sin\,\theta\,v_1\,sin\,\theta) = l\dot{\theta} \tag{12}$$

Simplifying Equation 12, one obtains Equation 13.

$$tan\,\varphi\,(v_1)(cos^2\theta + sin^2\theta) = l\dot{\theta} \tag{13}$$

With $cos^2\theta + sin^2\theta = 1$ in Equation 13 obtains Equation 14.

$$tan\,\varphi\,(v_1) = l\dot{\theta} \tag{14}$$

Solving Equation 14 for $\dot{\theta}$, one gets equation 15.

$$\dot{\theta} = \frac{v_1}{l} tan\,\varphi \tag{15}$$

Finally, using Equations 7, 8, 15 and considering the derivative of the steering angle, $\dot{\varphi}$, as a control input, the kinematic model can be described as shown in Equation system 16. Where v_2 is steering velocity, both v_1 and v_2 are controlled inputs.

$$\begin{aligned} \dot{\theta} &= \frac{v_1}{l} tan\,\varphi \\ \dot{\varphi} &= v_2 \end{aligned} \tag{16}$$

Control design

The objective of the controller is to ensure that the AutoNOMO-mini vehicle tracks a predefined trajectory. To develop the control system, from system 16, the Equation subsystem 17, given by $[\theta, \varphi]^{\mathrm{T}}$, will be employed. The control aim is to design a controller such that the orientation with respect to the x-axis, θ, globally tracks a reference θ_{ref}.

$$\begin{aligned} \dot{\theta} &= \frac{v_1}{l} tan\,\varphi \\ \dot{\varphi} &= v_2 \end{aligned} \tag{17}$$

PID-like controller

The PID controller is a cornerstone in control systems due to its robustness and ease of implementation. A PID controller is a control loop mechanism widely used in industrial control systems to regulate various process variables. PID stands for

Proportional, Integral, and Derivative, which are the three basic components used in the control algorithm. It is popular for its excellent performance in achieving asymptotic stability and precise control in steady-state conditions.

To this case, the control problem consists of designing a controller such that $\lim_{t\to\infty} \theta - \theta_{ref} = 0$. Hence, once the tracking error shown in Equation 18.

$$e = \theta - \theta_{ref} \tag{18}$$

And its dynamics are developed, one obtains Equation 19.

$$\dot{e} = \dot{\theta} - \dot{\theta}_{ref} \tag{19}$$

Replacing the value of $\dot{\theta}$ from Equation 17 in Equation 19, Equation 20 is obtained.

$$\dot{e} = \frac{v_1}{l} tan\, \varphi - \dot{\theta}_{ref} \tag{20}$$

Differentiating Equation 20, one obtains Equation 21.

$$\frac{d}{dt}\dot{e} = \ddot{e} = \frac{v_1}{l\, cos^2\, \varphi}\dot{\varphi} - \ddot{\theta}_{ref} \tag{21}$$

From subsystem 17, replacing $\dot{\varphi}$ with v_2, the steering velocity input, v_2, is obtained Equation 22. With $k_i > 0, k_p > 0, k_d > 0$.

$$v_2 = \frac{l}{v_1}\left(\dot{\theta}_{ref} - k_d\dot{e} - k_p e - k_i I_e\right) cos^2\, \varphi \tag{22}$$

In closed-loop, i.e. using Equation 22 into Equation 21, one obtains Equation 23.

$$\ddot{e} = -k_d\dot{e} - k_p e - k_i I_e \tag{23}$$

Under the following variable change $e_1 = e, e_2 = \dot{e}$, and proposing $Ie_1 = e_1$, the Equation 23 can be rewritten as: $\begin{pmatrix} \dot{Ie}_1 \\ \dot{e}_1 \\ \dot{e}_2 \end{pmatrix} = \begin{pmatrix} 0 & 1 & 0 \\ 0 & 0 & 1 \\ -k_i & -k_p & -k_d \end{pmatrix}\begin{pmatrix} Ie_1 \\ e_1 \\ e_2 \end{pmatrix}$. This matrix is Hurwitz with suitable k_i, k_p, k_d gains, such as ensuring that the tracking error $e = \theta - \theta_{ref}$ in Equation 18 exponentially converges to zero.

Sliding mode controller

The Sliding Mode Control (SMC) technique has two separate phases. The initial stage entails sliding, whereas the subsequent stage involves reaching. It is possible

to obtain two distinct types of control laws. These laws are the equivalent control and the switching control, respectively. SMC offers several benefits, including the ability to reject disturbances, resilience to changes in parameters, and a straightforward design of the controller. Although 'chattering' has its benefits, it can hinder SMC. Chattering, which refers to the undesired presence of oscillations with a specific frequency and amplitude, is created by switching the control portion [Utkin, 2006].

The control system aims to achieve a satisfactory control input v_2 to ensure that the output θ closely follows the predefined objective θ_{ref} over time, even in the presence of uncertainty and disturbances in the model. To determine the control input v_2, we will establish the tracking error similarly to equation18 as Equation 24.

$$e = \theta - \theta_{ref} \tag{24}$$

In this article, the sliding surface can be defined as shown in Equation 25.

$$s = \dot{e} + ce \tag{25}$$

Where $c > 0$ is a positive constant that represents the trajectory's rate of decay. To force $\dot{e}$ to reach $S = \{\dot{e} \in R: s = \dot{s} = 0\}$ in finite time, we begin by ensuring that $s(t)\dot{s}(t) < 0$ for all $t \geq 0$. For this, a Lyapunov function that must be positive and defined is proposed as Equation 26.

$$V(s) = \frac{1}{2}s^2 \tag{26}$$

By calculating the derivative of Equation 26, one gets Equation 27.

$$\dot{V}(s) = s\dot{s} = s(\ddot{e} + c\dot{e}) \tag{27}$$

Replacing $\dot{e}$ and $\ddot{e}$ from Equations 20 and 21 in Equation 27, Equation 28 is obtained.

$$\dot{V}(s) = s\left(\frac{v_1}{l\,cos^2\varphi}v_2 - \ddot{\theta}_{ref} + c\left(\frac{v_1}{l}tan\,\varphi - \dot{\theta}_{ref}\right)\right) \tag{28}$$

To ensure that the derivative of the Lyapunov function is negative definite $\dot{V}(s) < 0$, a control law that incorporates equivalent control and switching control is proposed in this paper, i.e. $v_2 = v_{2,eq} + v_{2,SW}$. Proposing the equivalent control in Equation 29.

$$v_{2,eq} = \frac{l\,cos^2\varphi}{v_1}c\left(\dot{\theta}_{ref} - \frac{v_1}{l}tan\,\varphi\right) \tag{29}$$

Substituting the equivalent control from Equation 29 into Equation 28, one obtains Equation 30.

$$\dot{V}(s) = s\left(\frac{v_1}{l\,cos^2\,\varphi}\,v_{2,SW} - \ddot{\theta}_{ref}\right) \tag{30}$$

The equivalent control cannot compensate for the control performance under the external disturbances inherent to the AutoNOMO-mini. Then, a second controller, $v_{2,SW}$, is designed to eliminate the effect of parametric uncertainties, i.e. Finally, substituting the switching control from Equation 31 into Equation 30, one obtains Equation 32.

$$v_{2,SW} = -\frac{l\,cos^2\,\varphi}{v_1}\big(Msign(s)\big);\; v_1 \geq 0 \tag{31}$$

$$\dot{V}(s) = s\left(-\ddot{\theta}_{ref} - Msign(s)\right) \tag{32}$$

Solving Equation 32, Equation 33 is obtained.

$$\dot{V}(s) = -M|s| - s\ddot{\theta}_{ref} \leq -\big(M + \ddot{\theta}_{ref}\big)|s| \tag{33}$$

Consequently, to guarantee that $\dot{V}(s)$ is negative definite, it is necessary to ensure that the gain M satisfies the condition in Equation 34.

$$M > sup_{t\to\infty}\left|\ddot{\theta}_{ref}\right| \tag{34}$$

3. Results

The controllers proposed in this work, the PID-like controller in Equation 22 and the sliding mode controller in Equations 29 and 31, have been subjected to two forms of testing on two platforms: i) numerical simulation using the mathematical model $[\theta, \varphi]^{\mathrm{T}}$ in subsystem 17 and Matlab–Simulink® software, and ii) real-time simulation using the AutoNOMO-mini vehicle (see Figure 1). The parameter values used in the simulations are presented in Table 1.

In this paper, it is assumed that the longitudinal velocity, v_1, remains constant for both simulation platforms under consideration. On the other hand, to measure the orientation of the scaled vehicle with respect to the x-axis, θ, an MPU6050 sensor is used, and the reference, θ_{ref}, is proposed as shown in Equation 35.

$$\theta_{ref}(t) = 0.5t \tag{35}$$

Table 1 System parameters.

Symbol	Description	Value / Unit
x, y	Cartesian coordinates	m
l	Distance between front and rear wheels	$0.27\ m$
θ	Orientation with respect to the x-axis	rad
φ	Steering angle	rad
v_1	Linear velocity	$0.82\ m/s$
v_2	Steering velocity	rad/s

Source: Authors

Numerical Simulations

As mentioned above, the numerical simulations were performed in Matlab–Simulink® software, which is a high–level language and interactive environment for numerical computation, visualization and programming. It enables engineers to analyze data, develop algorithms and create their own models and applications. Simulink® is a toolbox included in the Matlab® software for modeling, simulation and analysis of dynamic systems. It is a widely used tool in control engineering, signal processing for system simulation and model-based design.

The numerical simulations were performed using the PID-like controller in Equation 22 and the sliding mode controller, in Equations 29 and 31, into the mathematical model in subsystem 17, using the gains given in Table 2.

Table 2 Numerical Simulation: Gains used in controllers PID and the SMC.

Symbol	Description	Value
k_p	Proportional gain	10
k_i	Integral gain	10
k_d	Derivative gain	30
M	SMC gain	1.5
c	Rate of decay of the trajectory	1

Source: Authors

Figure 3 depicts the vehicle's trajectory given by both controllers. Figure 4 shows the vehicle's desired orientation, and θ obtained while applying the controllers.

In Figure 5, linear velocity can be observed. And finally, Figure 6 shows the control signal v_2 applied to the servomotor.

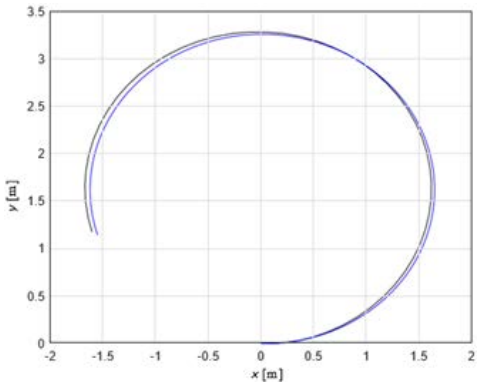

Source: authors

Figure 3 Numerical Simulation: Cartesian motion (x, y); PID (black) and SMC (blue).

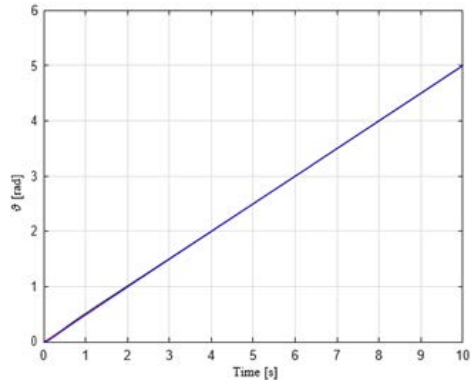

Source: authors

Figure 4 Numerical Simulation: Variable θ; PID (black), SMC (blue) and reference (red).

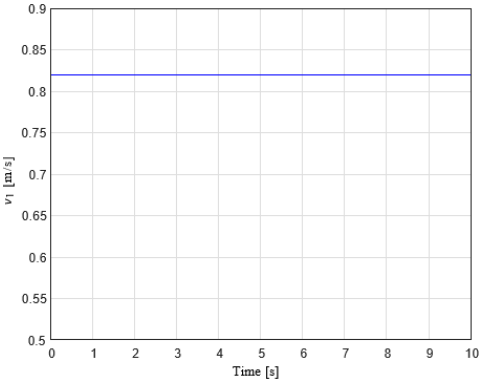

Source: authors

Figure 5 Numerical simulation: Longitudinal velocity v_1; PID (black) SMC (blue).

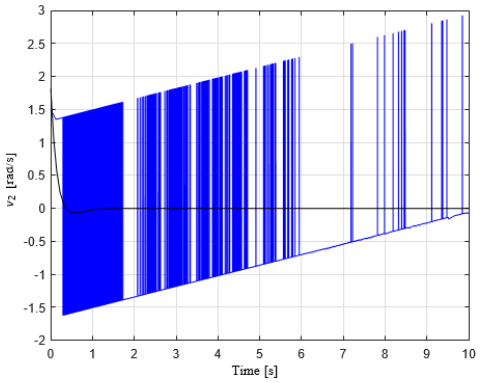

Source: authors

Figure 6 Numerical simulation: Input v_2; PID (black), SMC (blue).

Real-time results

The AutoNOMO-mini vehicle has several sensors, including a fish-eye camera, a kinetic system, a laser scanner, and an Inertial Measurement Unit (IMU). On the top of the car's body, the ELP 1080p fish-eye video camera is located pointing towards the ceiling. This camera is used to identify markers and simulate an indoor GPS system. The Intel RealSense SR300, a kinetic-type system, detects the lane and obstacles ahead of the vehicle. Additionally, the RPLIDAR A2 360, a rotating laser scanner, can also provide detection of obstacles around the vehicle. Two boards equip the vehicle. The main one is an Odroid XU4 board running Ubuntu Mate and Robot Operating System (ROS), while the other is an Arduino Nano. The Odroid directly connects both cameras and the RPLIDAR via USB. An XciteRc XLS-19s servomotor controls the steering, while a Faulhaber 2232 Brushless motor provides traction. The MPU6050 sensor is an IMU with 6 DoF that provides measurements of acceleration and angular velocity. The Arduino board controls this sensor. This board also connects to the Odroid via USB and manages the vehicle's actuators and control. For further details, refer to [Sanchez-Buelna, 2019].

The Real-time simulations were performed using the PID-like controller in Equation 22 and the sliding mode controller, in Equations 29 and 31, into the mathematical model shown in subsystem 17, using the gains given in Table 3.

Figure 7 displays the coordinates (x, y) of the vehicle's position in the inertial frame given by both controllers. The points of the trajectory are computed by integrating the signals obtained from the odometry sensor and encoder.

Table 3 Real-Time Simulation: Gains used in controllers PID and SMC.

Symbol	Description	Value
k_p	Proportional gain	10
k_i	Integral gain	100
k_d	Derivative gain	3
M	SMC gain	5.9
c	Rate of decay of the trajectory	1

Source: Authors

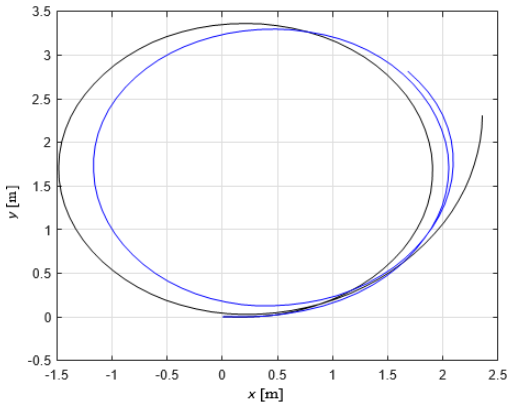

Source: authors

Figure 7 Real-Time simulation: Cartesian motion (x, y); PID (black) and SMC (blue).

Figure 8 illustrates the desired orientation of the AutoNOMO-mini, θ_{ref}, with respect to the x-axis and the real-time orientation θ of the vehicle obtained through the gyroscope over time. Figure 9 and Figure 10 display the behavior of both control signals v_1 and v_2, respectively. With v_2 as the steering velocity and v_1 as the linear velocity control signal, wich is calculated with the encoder.

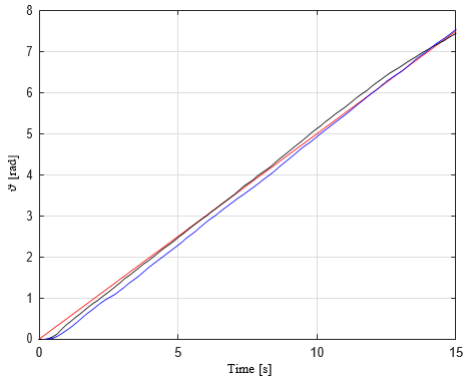

Source: authors

Figure 8 Real-Time simulation: Variable θ; PID (black), SMC (blue), and reference (red).

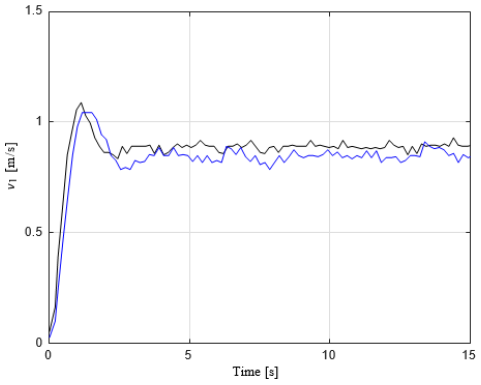

Source: authors

Figure 9 Real-Time simulation: Longitudinal velocity v_1; PID (black), SMC (blue).

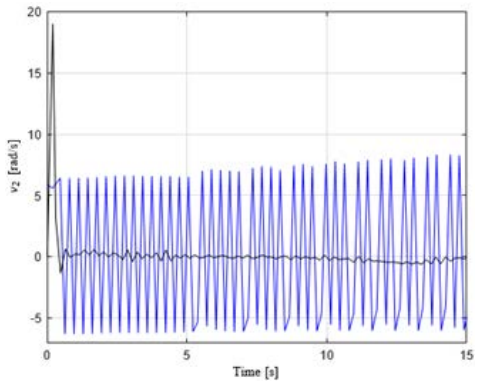

Source: authors

Figure 10 Real-Time simulation: Input v_2; PID-like controller (black), SMC (blue).

4. Discussion

From the results in Table 4, it is evident that the PID-like controller achieved a lower MAE (0.08869) and MSE (0.0056264) compared to the SMC, which had a higher MAE (0.13163) and MSE (0.012603). This suggests that the PID controller, known for its simplicity and ease of implementation, may be more suitable for environments with relatively low disturbance and where computational simplicity is prioritized.

Table 4 Metrics of performance.

Controller	MAE	MSE
PID-like controller	0.08869	0.0056264
SMC	0.13163	0.012603

Source: Authors

The PID controller's capacity to quickly and efficiently minimize the error between the actual and reference angle is evident from the lower error values.However, despite the higher error metrics, the SMC demonstrated enhanced robustness, particularly under conditions involving external disturbances and system uncertainties. This robustness is a well-known characteristic of SMC, attributed to its ability to reject bounded disturbances and handle model nonlinearities. In autonomous vehicle applications, where environmental uncertainties are common, the Sliding Mode controller's ability to maintain stability and accuracy under such conditions is critical. The chattering phenomenon, a known drawback of SMC, was also observed during the real-time experiments, though its impact on system performance was minimized through the application of appropriate control gains. The high gain settings used in the SMC ($M = 5.9$) helped to suppress disturbances but also led to increased system oscillations, contributing to the higher error metrics.

Another important observation is that while the PID-like controller was able to achieve a smoother control response, it lacked the robustness required for more complex, nonlinear vehicle dynamics. On the other hand, the SMC provided a more aggressive control response, which is better suited for nonlinear systems like the AutoNOMO-mini. This aggressive response, while increasing robustness, also resulted in higher energy consumption and control effort, as seen in the control signal plots (Figure 6 and 10), where the SMC exhibits more abrupt changes compared to the smoother control signal of the PID-like controller.

Therefore, the trade-offs between the simplicity and efficiency of the PID-like controller versus the robustness and disturbance rejection capability of the SMC must be carefully considered based on the specific application. For scenarios where computational simplicity and low error rates are critical, and the system operates in a relatively stable environment, the PID-like controller may be preferred. Conversely, for applications where external disturbances and nonlinearities play a significant role, the SMC offers a more suitable approach despite its higher complexity and control effort.

Finally, the real-time implementation of both controllers demonstrated that the SMC maintained better performance in handling the nonlinear dynamics of the

AutoNOMO-mini, especially in scenarios involving unmodeled dynamics or external disturbances. This makes the SMC more appropriate for advanced autonomous driving applications, where adaptability and robustness are prioritized over minimal steady-state error.

5. Conclusions

This study explored the effectiveness of two control strategies, a PID-like controller and a Sliding Mode Controller (SMC), for solving the trajectory tracking problem of a scaled autonomous vehicle, the AutoNOMO-mini. Both controllers were evaluated through numerical simulations in Matlab-Simulink and real-time experiments on the physical vehicle. The findings reveal that both controllers can achieve trajectory tracking; however, they exhibit distinct strengths and limitations, which are important to consider for practical implementations.

The PID-like controller exhibited good performance in tracking the desired trajectory under normal conditions. Its simple design and ease of implementation make it an excellent choice for systems where simplicity and computational efficiency are priorities. The controller's ability to minimize steady-state error while maintaining stability is noteworthy, as evidenced by its lower Mean Absolute Error (MAE) and Mean Squared Error (MSE) values.

On the other hand, the Sliding Mode Controller (SMC) is characterized by its superior robustness in the presence of disturbances and parametric uncertainties. This robustness is a key advantage of SMC, especially when controlling nonlinear systems such as the AutoNOMO-mini, where external factors can cause unpredictable changes in system behavior, making it a better option under challenging conditions. It's also worth noting that while SMC is more robust, it requires a higher control input, as indicated by the greater variations in control signals observed during the real-time experiments. This increased control effort, often accompanied by the phenomenon of chattering, can lead to higher energy consumption and potential wear on the vehicle's actuators.

In conclusion, the selection of the appropriate control strategy depends on the specific application requirements. For systems with relatively low disturbance and

where computational simplicity is valued, the PID-like controller is a better choice. On the other hand, for more complex systems that are subject to significant nonlinearities and external disturbances, the Sliding Mode Controller offers a more robust solution. Future work could involve the integration of adaptive control techniques or hybrid control strategies to combine the advantages of both controllers, aiming to achieve both robustness and efficiency in trajectory tracking for autonomous vehicles.

6. Bibliography and References

[1] De Luca, A., Oriolo, G., Samson, C. Feedback control of a nonholonomic car-like robot. Robot Motion Planning and Control, in Lecture Notes in Control and Information Sciences, vol. 229., pp. 171-253, Berlin, Heidelberg: Springer Berlin Heidelberg. 1998.

[2] Dong, X., Pei, H., Gan, M. Autonomous Vehicle Lateral Control Based on Fractional-order PID. 2021 IEEE 5th Information Technology, Networking, Electronic and Automation Control Conference (ITNEC), pp. 830-835, Xi'an, China. October, 2021.

[3] Farag, W. Complex Trajectory Tracking Using PID Control for Autonomous Driving. International Journal of Intelligent Transportation Systems Research, vol. 18, no. 2, pp. 356-366. May, 2020.

[4] Jiang, B., Li, J., Yang, S. An improved sliding mode approach for trajectory following control of nonholonomic mobile AGV. Scientific Reports, vol. 12, no 1, p. 17763. October, 2022.

[5] Kebbati, Y., Ait-Oufroukh, N., Vigneron, V., Ichalal, D., Gruyer, D. Optimized self-adaptive PID speed control for autonomous vehicles. IEEE 26th: International Conference on Automation and Computing (ICAC), pp. 1-6, Portsmouth, United Kingdom. September, 2021.

[6] Kong, J., Pfeiffer, M., Schildbach, G., Borrelli, F. Kinematic and dynamic vehicle models for autonomous driving control design. 2015 IEEE Intelligent Vehicles Symposium (IV), pp. 1094-1099, Seoul, South Korea. June, 2015.

[7] Milani, S., Khayyam, H., Marzbani, H., Melek, W., Azad, N., L., Jazar, R. N. Smart Autodriver Algorithm for Real-Time Autonomous Vehicle Trajectory Control. IEEE Transactions on Intelligent Transportation Systems, vol. 23, pp. 1984-1995. March, 2022.

[8] Rajasekhar, M. V., Jaswal, A. K. Autonomous vehicles: The future of automobiles. 2015 IEEE International Transportation Electrification Conference (ITEC), pp. 1-6, Chennai, India. 2015.

[9] Sabiha, A. D., Kamel M. A., Said, E., Hussein, W. M. ROS-based trajectory tracking control for autonomous tracked vehicle using optimized backstepping and sliding mode control. Robotics and Autonomous Systems, vol. 152, p. 104058. June 2022.

[10] Sanchez-Buelna, L., Acosta-Lua, C., Sanchez-Morales, M. E., Navarrete-Guzman, A., Di-Gennaro, S. Nonlinear control with experimental identification applied to an scale electric vehicle. 2019 IEEE International Autumn Meeting on Power, Electronics and Computing (ROPEC), pp. 1-6, Ixtapa, Mexico. November, 2019.

[11] Sekban, H. T., Basci, A. Designing New Model-Based Adaptive Sliding Mode Controllers for Trajectory Tracking Control of an Unmanned Ground Vehicle. IEEE Access, vol. 11, pp. 101387-101397. 2023.

[12] Tiwari, T., Agarwal, S. Etar, A. Controller Design for Autonomous Vehicle. IEEE: 2021 International Conference on Advances in Electrical, Computing, Communication and Sustainable Technologies (ICAECT), pp. 1-5, Bhilai, India. February, 2021.

[13] Utkin, V., Hoon, L. Chattering Problem in Sliding Mode Control Systems. International Workshop on Variable Structure Systems, pp. 346-350, Alghero, Sardinia. 2006.

[14] Zhejun, H., Li, H., Li, W., Liu, J. Huang, C., Yang, Z., Fang, W. A New Trajectory Tracking Algorithm for Autonomous Vehicles Based on Model Predictive Control. Sensors, vol. 21, p. 7165. October, 2021.